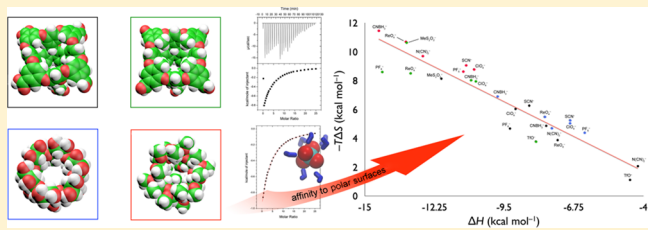


The Thermodynamics of Anion Complexation to Nonpolar Pockets

Matthew R. Sullivan,^{†,§} Wei Yao,^{†,§} Du Tang,[‡] Henry S. Ashbaugh,^{‡,¶} and Bruce C. Gibb*,^{†,¶}[†]Department of Chemistry and [‡]Department of Chemical and Biomolecular Engineering, Tulane University, New Orleans, Louisiana 70118, United States

Supporting Information

ABSTRACT: The interactions between nonpolar surfaces and polarizable anions lie in a gray area between the hydrophobic and Hofmeister effects. To assess the affinity of these interactions, NMR and ITC were used to probe the thermodynamics of eight anions binding to four different hosts whose pockets each consist primarily of hydrocarbon. Two classes of host were examined: cavitands and cyclodextrins. For all hosts, anion affinity was found to follow the Hofmeister series, with associations ranging from 1.6–5.7 kcal mol⁻¹. Despite the fact that cavitand hosts **1** and **2** possess intrinsic negative electrostatic fields, it was determined that these more enveloping hosts generally bound anions more strongly. The observation that the four hosts each possess specific anion affinities that cannot be readily explained by their structures, points to the importance of counter cations and the solvation of the “empty” hosts, free guests, and host–guest complexes, in defining the affinity.



INTRODUCTION

Although Franz Hofmeister’s seminal studies into how salts affect proteins dates back to 1888, there are still countless open questions pertaining to how salts affect water and aqueous solutions of solutes.^{1–3} Hofmeister’s early work observed that certain salts were capable of causing proteins to precipitate, while others caused the protein to become more soluble. For example, salting-out salts such as ammonium sulfate are the most common additives for protein crystallization,⁴ while salting-in salts such as sodium thiocyanate are most often found to (partially) denature proteins and increase their solubility.⁵ By this metric of solubility, Hofmeister observed the continuum of anions now named after him (Figure 1), and since that time, this Hofmeister series has been observed in over 40 physicochemical measurements of aqueous solutions.⁶

The first picture to emerge of the Hofmeister effect was based mostly on macroscale measurements^{7–19} and centered on the idea that salts affect solute properties *indirectly* by changing the structure of water.²⁰ More recently, however, the arrival of more powerful analytical and computational tools have led to a shifting in understanding. For example, data from a suite of spectroscopic techniques suggests that salts do not significantly influence the structure of bulk water and therefore are unlikely to *indirectly* influence cosolute molecules or macromolecules.^{21–29} More importantly, data from recent studies at the air–water interface,^{30–40} oil–water interface,^{41–43}

and macromolecule–water interface^{44–54} all suggest that polarizable anions—those that can more readily undergo partial desolvation—interact directly with molecules and macromolecules. Correspondingly, one important and open question arising from this is how do these anion–solute interactions induce Hofmeister effects, such as anion dependent protein denaturation, in (macro)molecules?

Whether an anion can associate with a (macro)molecule depends on the intrinsic anion–solute interaction, the intrinsic ion pairing of the salt,^{55–58} and how strongly all species are solvated. Regarding the latter, in general terms, the further an anion lays toward the salting-in end of the Hofmeister series, the more weakly it is solvated.⁵⁹ However, our understanding of the preferred geometries, thermodynamics, and spectroscopic signatures of hydrated anions ($X^-(H_2O)_n$) is limited to indirect measurements of dilute solutions,⁶⁰ and general observations such as the stepwise removal of solvating waters only becomes energetically demanding with the last few waters.^{61–64} Even more problematic, the greater diversity within (macro)molecule solutes means that solvation of these surfaces is exceedingly complex. General descriptors of solute surfaces, such as convex, planar, and concave, can be readily invoked to define solvation types,⁶⁵ but it remains unclear if specific subtypes of hydration—for example, the chiral spine of hydration in DNA⁶⁶—are common to other topologies and/or individual families of functional groups.

The strength of an interaction between an anion and a (macro)molecule is also dependent on the intrinsic ion–solute interaction, and in this regard, it is undoubtedly concave solute surfaces that offer the strongest affinity; independent of the net electrostatic potential at the surface and regardless of their constituent atoms, concave surfaces allow the maximum number of noncovalent interactions between solute and anion. Protein surfaces are of course replete with gullies, hollows, and concavities, and along with positively charged residues,⁶⁷ arguably the most familiar anion recognition sites on

Received: December 13, 2017

Revised: January 10, 2018

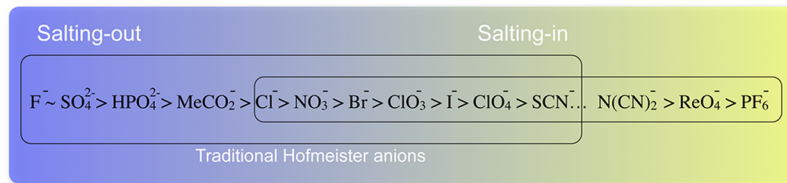


Figure 1. Traditional Hofmeister series of anions and potential candidate anions for extending the salting-in end of the continuum.

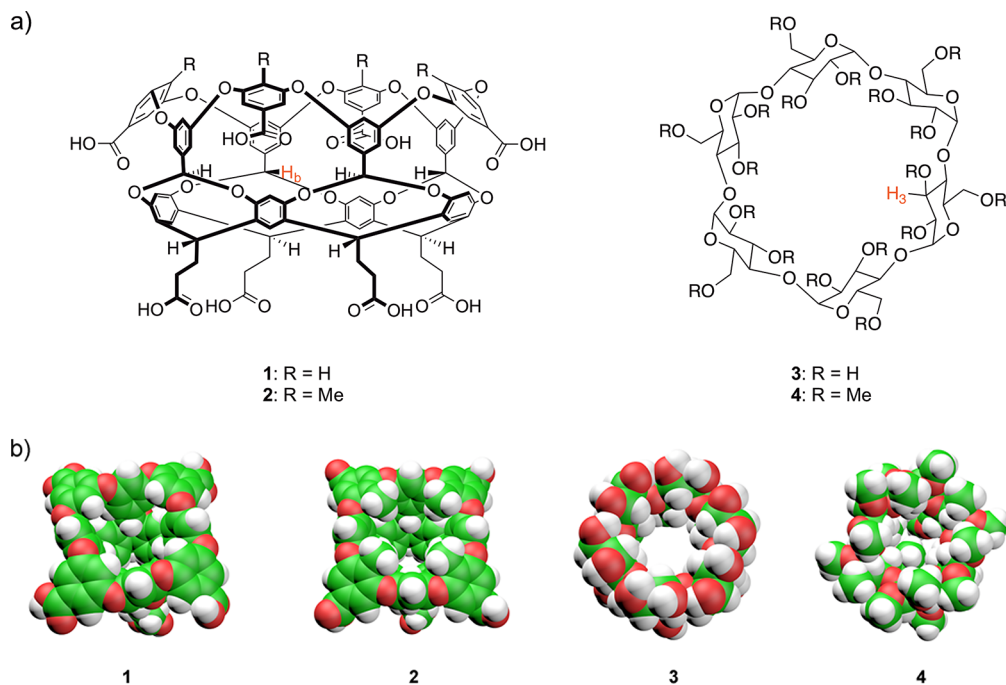


Figure 2. Hosts used in this study. (a) Chemical structure representations. Atoms used for ¹H NMR spectroscopy experiments to determine binding constants (K_a) are highlighted in red. (b) Space filling models of hosts 1–4, looking down into the cavity of each.

their surfaces are the triple hydrogen-bonding Nest (three \times amide N–H) and C $^{\alpha}$ NN (alpha C–H and two \times N–H) motifs.^{68,69} That noted, there is also growing evidence of direct supramolecular interactions between polarizable anions and nonpolar surfaces, not only at the air–water interface^{30–40} and the oil–water interface^{41–43} but also at nonpolar surfaces of macromolecules.^{70–77} Thus, it would appear that with the exception of those residing within strongly negative electrostatic potentials, most concavities on the surface of a protein are conceivably sites for the recognition of poorly hydrated anions. Furthermore, in assessing potential binding sites, there are also those *near* to the surface of a protein. In the solid state, the average globular protein displays approximately 4.4 cavities per 100 amino acids large enough to bind a water molecule.⁷⁸ These are found most frequently at a depth of 2.50–3.60 Å from the surface, and it is not difficult to envisage that in the solution state these sites—hydrated or not—are available to bind polarizable species such as thiocyanate (SCN[−]).

In considering all these different potential anion-binding sites in globular proteins, it is important to note that they need not be of particularly high affinity; many Hofmeister effects, including denaturation, are observed at molar concentrations. Rather, the large number and variety of these pseudo-specific binding sites must sum in ways that make each protein unique yet still generally follow the Hofmeister effect. It is therefore important to determine the extent to which different anion-binding sites, each with their own unique combination of

Coulombic interactions, hydrogen bonding, and van Der Waals interactions, contribute to anion binding, the denaturation of proteins, and Hofmeister effects in general. As a step toward understanding anion–nonpolar surface interactions, in this paper we ask the question, how does the shape of the nonpolar binding site affect anion affinity?

Our own understanding of how anions interact with nonpolar surfaces was triggered by a study of how the complexation of organic guests to host 1 (octa-acid (OA), Figure 2) is affected by salts.^{79–82} We showed that those anions expected to weaken the hydrophobic effect did indeed attenuate amphiphile binding to 1 and that this was because of anion affinity for the nonpolar pocket that led to competitive binding. Building on this, we have also observed that the binding of polarizable anions to the nonpolar pocket of 1 is itself subject to the Hofmeister effect. Thus, the association of perchlorate (ClO₄[−]) to the nonpolar pocket of 1—a phenomenon that weakens the apparent affinity of amphiphiles to the host—can itself be attenuated with salting-in salts and augmented with salting-out salts.⁸² This study revealed that almost all of the changes in ΔG° of ClO₄[−] complexation in response to the nature and concentration of an added salt could be attributed directly to salt interactions with the host. Specifically, a weak, omnipresent cation binding to the carboxylates decreased the net negative charge of the host and increased ClO₄[−] affinity, and for polarizable anions such as

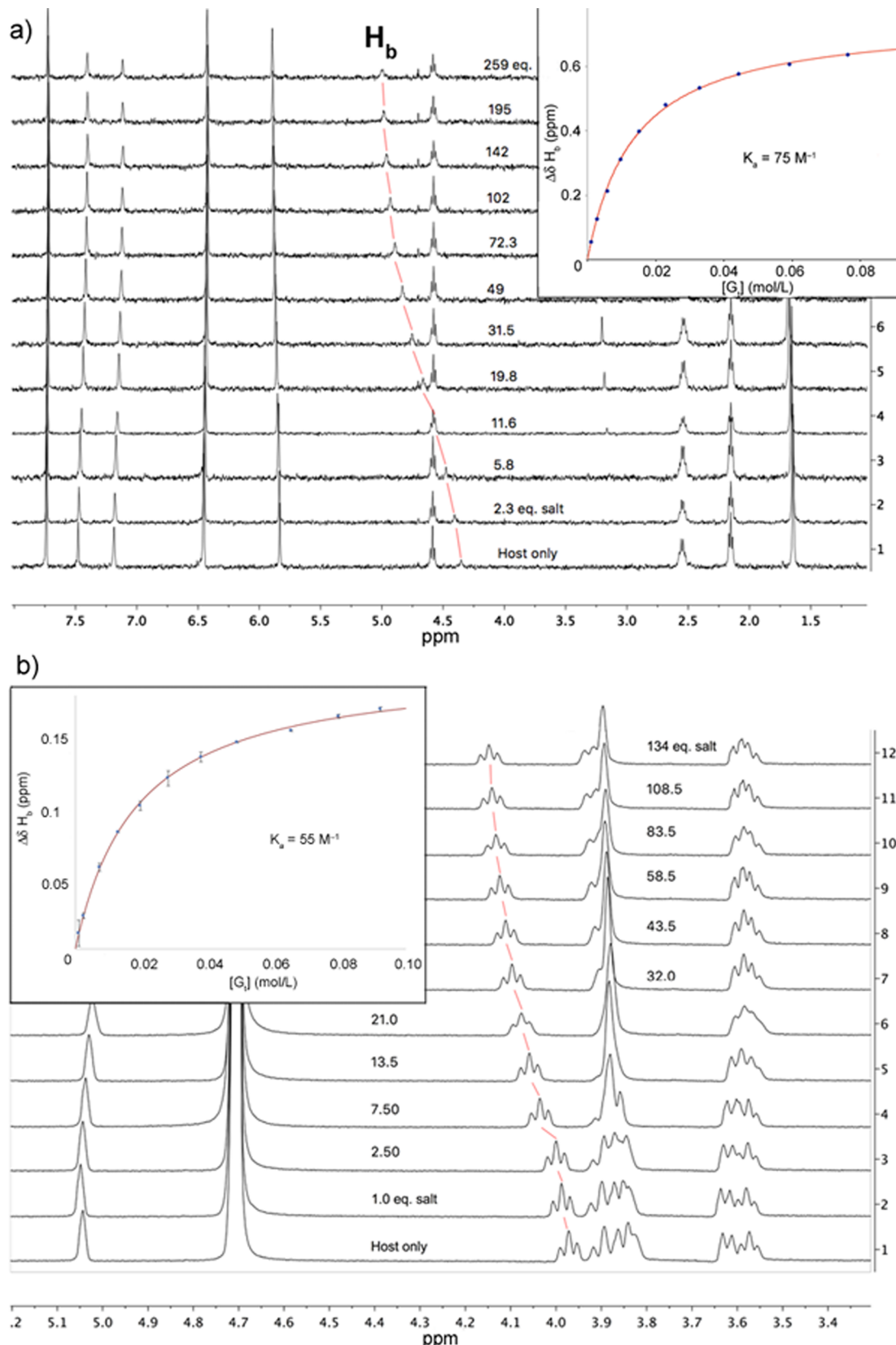


Figure 3. (a) Stack of ^1H NMR spectra from the titration of NaMeSO_2S (350 mM) into a solution of 0.5 mM **2** (10 mM phosphate buffer, $\text{pH} = 11.3$, 25°C). Inset: the resultant binding isotherm fit to the 1:1 model. (b) Stack of ^1H NMR spectra from the titration of NaReO_4 (300 mM) into a solution of 1 mM **3** (10 mM phosphate buffer, $\text{pH} = 11.3$, 25°C). Inset: the resultant binding isotherm fit to the 1:1 model.

SCN^- , a counteracting and generally stronger interaction decreased ClO_4^- affinity via direct competition for the pocket.

To improve our understanding of how the structure of a host contributes to anion binding, we discuss here four hosts with

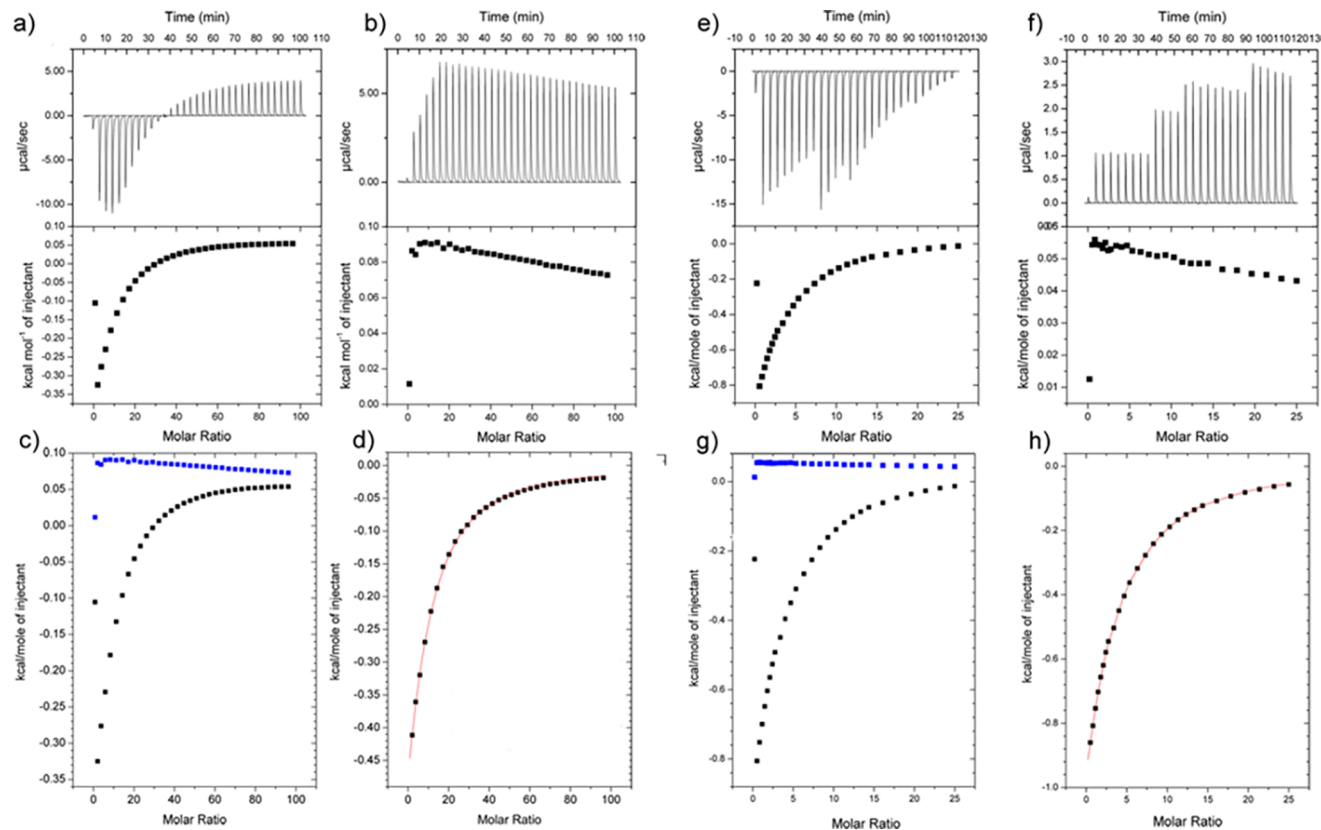


Figure 4. (a–d): ITC data for the complex formed between **2** and ClO_4^- at 25 °C; (a) **2** (0.5 mM) titrated with NaClO_4 (350 mM) in phosphate buffer (50 mM, pH = 11.7); (b) NaClO_4 into buffer alone; (c) an overlay of parts a and b; (d) final binding curve obtained by subtraction of part b from part a; (e–h): ITC data for the complex formed between **3** and $\text{N}(\text{CN})_2^-$ at 25 °C; (e) **3** (0.5 mM) titrated with $\text{NaN}(\text{CN})_2$ (150 mM) in phosphate buffer (50 mM, pH = 11.7); (f) $\text{NaN}(\text{CN})_2$ into buffer alone; (g) an overlay of parts e and f; (h) final binding curve obtained by subtraction of part f from part e.

different shapes and types of pockets composed primarily of hydrocarbon. We use isothermal titration calorimetry (ITC) and NMR spectroscopy to measure the thermodynamics of binding of polarizable (salting-in) anions to tetra-*endo*-methyl octa-acid cavitand **2** (TEMOA),^{83,84} α -cyclodextrin (α -CD) **3**, and permethylated α -cyclodextrin (PM- α -CD) **4** (Figure 2)⁸⁵ and compare these to anion binding to OA **1**.⁸¹ We selected these hosts based on their availability (known synthetic hosts that bind anions in water are quite rare) and because these two classes of host possess very different kinds of pockets that might reveal the generality of anion binding to nonpolar surfaces. In terms of the nature of the salts used, the focus was on sodium salts; the important factor of the nature of the cation was not addressed here.

RESULTS

¹H NMR Spectroscopy and ITC Titrations with Hosts 1–4. Both ¹H NMR spectroscopy and ITC were used to probe anion affinity to the hosts. As salting-out anions such as chloride (Cl^-) were not observed to bind to host **1**,⁸¹ we focused here on salting-in salts that are thought to associate with nonpolar surfaces (vide supra). To ensure good data collection, we augmented this list (Figure 1) with common, large, and charge diffuse anions that might be expected to associate even more strongly than typical salting-in anions such as perchlorate (ClO_4^-). Of the 11 salts examined, fluoride (F^-) and Cl^- were not observed to bind to any of the hosts by either technique, and bromide (Br^-) bound too weakly to all hosts to

provide reliable data. The remaining anions, SCN^- , ClO_4^- , triflate (TFO^-), dicyanamide ($(\text{CN})_2\text{N}^-$), hexafluorophosphate (PF_6^-), perrenate (ReO_4^-), cyanoborohydride (CNBH_3^-), and methanethiosulfonate (MeSO_2S^-), were observed to bind to at least one of the hosts using at least one technique. Typical NMR spectroscopy data, from the titration of host **2** with MeSO_2S^- and host **3** with ReO_4^- , are shown in Figure 3. For hosts **1** and **2**, the signal from the four inward pointing acetal protons (H_b , see Figure 2) was monitored during titration, whereas for hosts **3** and **4**, the signal from the inward pointing H_3 atoms was used. The maximal $\Delta\delta$ values for the H_3 signal were generally somewhat smaller than the corresponding shift of H_b , but in both cases, anion complexation induced the expected downfield signal shifts. These changes were attributed purely to anion association; changes in the magnetic susceptibility of the solvent due to increasing ionic strength⁸⁶ have previously been noted to be small at the ionic strengths attained at the end point of the titrations reported here. Consequently, the shift data as a function of the host–guest ratio fit well to a 1:1 model using nonlinear least-squares protocols (Figure 3, insets).

Representative ITC titration data, for ClO_4^- binding to host **2** and $(\text{CN})_2\text{N}^-$ binding to host **3**, are shown in Figure 4. In all cases, the modified procedures defined by Turnbull⁸⁷ and Tellinghuisen⁸⁸ were followed to account for relatively small Wiseman parameters c ($c = [\text{Host}] \times K_c$). Thus, variable injection volumes were used to titrate a large excess of salt to ensure host saturation at the end of the titration. Additionally,

Table 1. Thermodynamic Data for the Binding of Anions (All Sodium Salts) to Hosts 1 and 2^a

host	guest	K_a (M ⁻¹)		ΔG° (kcal mol ⁻¹)	ΔH° (kcal mol ⁻¹)	$-T\Delta S^\circ$ (kcal mol ⁻¹)
		NMR ^b	ITC ^c			
OA (1) ^d	N(CN) ₂ ⁻	10	37	-2.15	-4.22	2.07
	CNBH ₃ ⁻	67	152	-2.98	-7.84	4.87
	ReO ₄ ⁻	322	371	-3.51	-7.39	3.88
	PF ₆ ⁻	1560	2303	-4.59	-9.27	4.68
	SCN ⁻	33	44	-2.24	-8.51	6.27
	TfO ⁻	67	314	-3.41	-4.53	1.12
	CH ₃ SO ₂ S ⁻	391	660	-3.85	-11.98	8.14
	ClO ₄ ⁻	95	160	-3.01	-9.05	6.04
TEMOA (2)	N(CN) ₂ ⁻	9	--	--	--	--
	CNBH ₃ ⁻	103	104	-2.75	-10.81	8.03
	ReO ₄ ⁻	2391	2663	-4.67	-13.19	8.51
	PF ₆ ⁻	15 306	15 133	-5.69	-14.31	8.60
	SCN ⁻	14	--	--	--	--
	TfO ⁻	1073	1837	-4.45	-8.25	3.78
	CH ₃ SO ₂ S ⁻	75	98	-2.71	-13.35	10.64
	ClO ₄ ⁻	58	90	-2.67	-10.62	7.95

^aThe average of two or three individual experiments with error <10% (standard deviations shown in Supporting Information). ^b25 °C, 10 mM sodium phosphate D₂O buffer, pD = 11.6. ^c25 °C, 50 mM sodium phosphate buffer, pH = 11.7. ^dData for host 1 reproduced from reference 81, with the exception of PF₆⁻ data, which was redetermined here due to errors in the initial measurement (see text).

Table 2. Thermodynamic Data for the Binding of Anions (All Sodium Salts) to Hosts 3 and 4^a

host	guest	K_a (M ⁻¹)		ΔG° (kcal mol ⁻¹)	ΔH° (kcal mol ⁻¹)	$-T\Delta S^\circ$ (kcal mol ⁻¹)
		NMR ^b	ITC ^c			
α CD (3)	N(CN) ₂ ⁻	149	140	-2.93	-7.62	4.70
	CNBH ₃ ⁻	106	124	-2.85	-9.76	6.90
	ReO ₄ ⁻	55	58	-2.41	-7.90	5.49
	PF ₆ ⁻	20	26	-1.92	-6.32	4.39
	SCN ⁻	15	16	-1.65	-6.90	5.25
	TfO ⁻	6	--	--	--	--
	CH ₃ SO ₂ S ⁻	--	--	--	--	--
	ClO ₄ ⁻	8	23	-1.86	-6.90	5.04
PM α CD (4)	N(CN) ₂ ⁻	33	160	-3.01	-12.71	9.70
	CNBH ₃ ⁻	66	151	-2.99	-14.45	11.46
	ReO ₄ ⁻	84	92	-2.68	-13.38	10.70
	PF ₆ ⁻	43	64	-2.48	-11.11	8.63
	SCN ⁻	16	26	-1.94	-11.00	9.06
	TfO ⁻	20	--	--	--	--
	CH ₃ SO ₂ S ⁻	--	--	--	--	--
	ClO ₄ ⁻	8	25	-1.91	-10.69	8.78

^aThe average of two or three individual experiments with error <10% (standard deviations shown in Supporting Information). ^b25 °C, 10 mM sodium phosphate D₂O buffer, pD = 11.6. ^c25 °C, 50 mM sodium phosphate buffer, pH = 11.7.

based on the 1:1 fitting observed from the NMR data, the stoichiometry parameter N was set to 1.0 during curve fitting of the ITC data. Furthermore, in some experiments, heats of dilution were significant when the salt was titrated into buffer solution in the absence of host. Consequently, in all cases, reference titrations in the absence of host were carried out and subtracted from the host–guest titration data. In all cases, this resulted in excellent fits to the 1:1 model.

Because of the slightly different ionic strengths of the solutions required for the NMR spectroscopy and ITC experiments, K_a values obtained from the two techniques were found to differ somewhat. Specifically, in general, the higher ionic strength of the ITC experiments (50 versus 10 mM sodium phosphate buffer) led to slightly stronger affinities, particularly for charged hosts **1** and **2**. This is primarily attributed to the fact that their net charge is influenced by

differences in I and is fully consistent with our previous work with these hosts (vide infra).⁸²

Table 1 shows the complexation data of TEMOA **2** alongside the previously reported data for OA **1**. Regarding the latter, in crosscheck ITC experiments, we determined that the earlier data for PF₆⁻ was incorrect. This was due to trace hydrolysis of the salt, leading to solutions that exceeded the buffering capacity of the sodium phosphate buffer. As a result, small pH differences between the solutions in the cell and the injector resulted in the collected data containing a small background heat of protonation(s). The NaPF₆ data shown in **Table 1** corrects this error.

The measurable anion affinity for the pocket of **1** ranges from -2.15 to -4.59 kcal mol⁻¹ (av. = -3.22 kcal mol⁻¹), whereas the corresponding range for **2** is -2.67 to -5.69 kcal mol⁻¹ (av. = -3.82 kcal mol⁻¹). Moreover, overall, binding to **2** is

considerably more exothermic and more entropically penalized than binding to **1**. Thus, the range in ΔH for binding to host **1** was -4.22 to -11.98 kcal mol $^{-1}$ (av. -7.85 kcal mol $^{-1}$), whereas in the case of **2**, the range was -8.25 to -14.31 kcal mol $^{-1}$ (av. -11.75 kcal mol $^{-1}$). Correspondingly, the range in $-T\Delta S$ for anion binding to **1** was from 1.12 to 8.14 kcal mol $^{-1}$ (av. $= 4.63$ kcal mol $^{-1}$), whereas for **2**, the range was 3.78 to 10.64 kcal mol $^{-1}$ (av. $= 7.96$ kcal mol $^{-1}$).

The anion affinity data from spectroscopy and ITC for α -cyclodextrin **3** and PM- α -CD **4** are presented in Table 2. In contrast to hosts **1** and **2**, the affinities measured by the two different techniques are similar; the exceptions being the binding of dicyanamide and CNBH $_3^-$. We attribute these smaller differences to the fact that **3** and **4** are uncharged and that they are therefore less influenced by differences in the ionic strength.

In general, ITC reveals that anion affinities for hosts **3** and **4** are weaker than those observed for cavitands **1** and **2**, and it is the parent cyclodextrin **3** that displays the weakest affinities for the different anions investigated. Thus, in the case of host **3**, anion affinity ranged from -1.65 to -2.93 kcal mol $^{-1}$ (av. $= -2.27$ kcal mol $^{-1}$), whereas in the case of **4**, it ranged from -1.91 to -3.01 kcal mol $^{-1}$ (av. $= -2.50$ kcal mol $^{-1}$). There are striking differences between the enthalpy and entropy contributions to anion affinity for **3** and **4**. Thus, the range in ΔH for binding to host **3** was from -6.32 to -9.76 kcal mol $^{-1}$ (av. $= 7.57$ kcal mol $^{-1}$), whereas in the case of **4**, the range was from -10.69 to -14.45 kcal mol $^{-1}$ (av. $= -12.22$ kcal mol $^{-1}$). Correspondingly, the range in $-T\Delta S$ for anion binding to **3** was from 4.39 to 6.90 kcal mol $^{-1}$ (av. $= 5.30$ kcal mol $^{-1}$), whereas for **4**, the range was from 8.78 to 11.46 kcal mol $^{-1}$ (av. $= 9.72$ kcal mol $^{-1}$).

Calculated Electrostatic Potentials for the Cavities of **1 and **2**.** OA **1** and TEMOA **2** are negatively charged but are still capable of binding anions. In an effort to understand why this is so, as well as to understand the difference between the binding profiles of these hosts, the electrostatic potentials within and around **1** and **2** were determined in the gas phase.

To achieve this, we obtained partial atomic charges for OA **1** and TEMOA **2** in the 6 $^-$ state (two carboxylic acids at the feet remaining protonated; the likely predominant species at pH = 11.6) by fitting to AM1-BCC⁸⁹ potentials following geometry optimization as described previously.⁹⁰ Given the rotational symmetry about the C₄-axis of the host, we evaluated the electrostatic potential about the hosts in cylindrical coordinates centered on the symmetry axis and averaged the potential over the azimuthal angle θ . The angularly averaged vacuum potentials for the two cavitands are directly compared in Figure 5 as a function of the cylindrical radial distance r and vertical rise z .

■ DISCUSSION

Hosts and Guests. Hosts **1**,⁸¹ **2**,^{83,84} and **4**⁸⁵ were synthesized as previously reported. Host **3** was obtained from commercial sources. We examined the complexation of eight polarizable anions to the three hosts **2–4** in order to compare their affinities to that displayed by **1**. The parent octa-acid (OA) **1** is a bowl-shaped amphiphile made water-soluble by eight carboxylates on its outer coat (four at its rim and four at its pendent “feet”). These are relatively remote from the primary binding site, an ostensibly nonpolar concavity defined by the 12 aromatic rings that make up the bulk of the structure. This binding site is ~ 8 Å wide at its open portal (the top of the

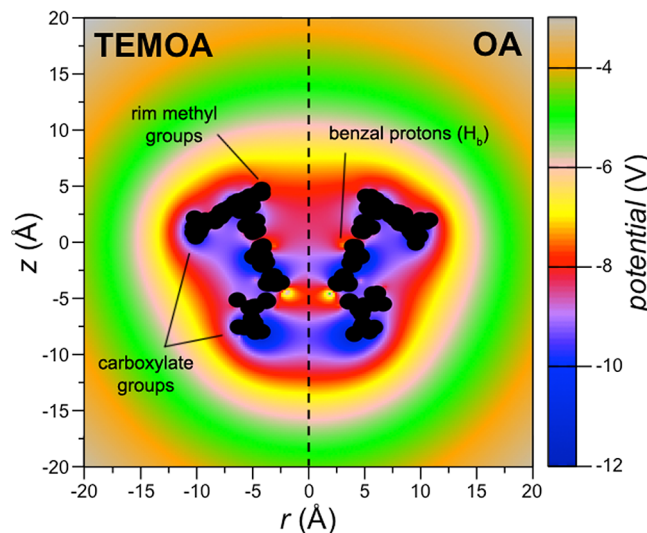


Figure 5. Cylindrically averaged electrostatic potential as a function of the radial distance r from the C₄-axis of symmetry and vertical rise z for the cavitands **1** and **2** in vacuum. The potentials are averaged about the azimuthal angle θ . The results for OA **1** (right) and TEMOA **2** (left) are separated by the dashed dividing center line. The color scale for the electrostatic potential is reported in the legend to the right. The black shadow on the diagram represents the positions of the cavitand heavy atom, cylindrically rotated about the symmetry axis to obscure the electrostatic poles at the centers of the atoms. The positions of the methyl groups (of TEMOA **2**), the benzal hydrogens, and the carboxylates are shown for reference.

host as depicted in Figure 2) and ~ 8 Å deep. Importantly, it is closed off at the base; guest entry—be it water, an anion, or a nonpolar guest—must be through the aforementioned portal. TEMOA **2** only differs from OA **1** by possessing four methyl groups that project from the rim of the host and narrow the portal slightly (Figure 2b). These do not represent a direct steric barrier to entry or egression for the anions discussed here, the largest of which is TfO $^-$ (vol. = 84 Å 3). Only in the case of highly rotund guests do these methyl groups impede binding kinetics and attenuate affinity. For example, Z-4-bromo-adamantane-1-carboxylate (vol. = 205 Å 3) binding to **1** is over 5 orders of magnitude stronger than that to **2**.⁸¹

For an alternative form of nonpolar pocket CDs, **3** and **4** were selected. Hosts **3** and **4** can be viewed as being minimalist, weak binders of anions; they are neither charged or project any functionality into the core pocket, and they possess two portals for entry and egression. Moreover, being alkylated at the rim, **4** is completely devoid of hydrogen donor —OH groups that might contribute to anion recognition.

CDs differ in two fundamental ways from cavitands **1** and **2**. The walls of the nonpolar pockets of **3** and **4** are saturated rather than unsaturated, suggesting they are slightly more polarizable than **1** or **2** and can form stronger van der Waals interactions. More importantly perhaps, the solid-state structure of **4** notwithstanding,⁹² the gross form of **3** and **4** are toroidal, whereas hosts **1** and **2** are bowl-shaped. Based on this topological difference, the observed stronger binding of amphiphiles to **1** versus **3**,^{91,93,94} as well as molecular dynamics simulations probing the structure and thermodynamics of waters within the pocket of **1**⁹⁵ and **3**,⁹⁶ we surmise that the pockets of **1** and **2** are less well solvated than those of the cyclodextrins. This is, however, hard to determine spectroscopically. Solvatochromic probes such as 8-anilinonaphthalene-1-

sulfonic acid (ANS) suggest that the polarity of the binding pocket of **4** approximates to ethanol, whereas that of **3** is equivalent to a 3:1 methanol/water mixture,^{97,98} but the very different constitutions of cavitands **1/2** and CDs **3/4** make data from partially included fluorescent probes hard to interpret.⁹⁹ Moreover, the common dyes that can theoretically be fully included within **1** or **2**, e.g., 2,3-diazabicyclo[2.2.2]oct-2-ene (DBO), would trigger dimerization and formation of the 2:1 and 2:2 host–guest capsular complex.¹⁰⁰

Of the two α -CDs considered here, α -CD **3** has been previously examined for its small anion-binding properties.¹⁰¹ Indeed, the binding of I_3^- to **3** dates back to 1958¹⁰² and was itself inspired by the iodine test (I_3^- binding to starch).¹⁰³ However, probing small anion binding to α -CD **3** (and β -CD) has frequently been indirect, e.g., with conductance,¹⁰⁴ potentiometry,¹⁰⁵ and polarography,¹⁰⁶ and where more direct techniques have been applied such as 1H NMR,¹⁰⁶ only limited van't Hoff analysis has been applied.⁸⁶ To our knowledge, only in one case has calorimetry been applied to small anion binding to α -CD **3**¹⁰⁷ and only for three of the anions discussed here: ClO_4^- , PF_6^- , and TfO^- . To ensure consistency with our data, and because of the different solution conditions used, we repeated the ITC data for these three anions.

The list of guests chosen included the traditional “Hofmeister anions”: F^- , Cl^- , Br^- , I^- , ClO_4^- , and SCN^- , but this was augmented by a number of other anions that were noted to strongly associate, the majority of which are typically classified by organic and organometallic chemists as, “non-coordinating anions”. Specifically, the following anions were also included in this study: TfO^- , $N(CN)_2^-$, PF_6^- , ReO_4^- , $CNBH_3^-$, and $CH_3SO_2S^-$. Our screening demonstrated that these possess strong coordinating properties in water and therefore would have stronger (and therefore more easily measured) salting-in properties than anions such as SCN^- . This wider pool of binding anions also provides a broader picture an anion–nonpolar surface affinity.

Electrostatic Potential Calculations for Hosts **1** and **2**.

Hosts OA **1** and TEMOA **2** are only readily water-soluble under basic conditions. As a result, the work described here (as well as our previous Hofmeister studies^{79–82} with OA **1**) was carried out at pH ≈ 11.6, where **1** is a polyanion. As a result, the binding pocket of both **1** and **2** are expected to have a net, negative electrostatic potential. Figure 5 confirms this, showing the cross section of the cylindrically averaged electrostatic potential for OA **1** and TEMOA **2** in the 6^- state (the likely predominant species at pH = 11.6). These maps do not include the effects of counterions or water but rather represent the intrinsic electrostatic potential fields generated by each host. Because of charge and dielectric reasons respectively, both counteranions and water are expected to greatly attenuate the electrostatic potential field. As Figure 5 reveals, the electrostatic potential within the pocket of both hosts is quite heterogeneous, varying from -8 V at the portal, to -12 V deeper in the pocket, up to -7 V at the very base of the binding site. We believe that there are several factors contributing to this heterogeneity. First, the electrostatic potential within the pocket increases from -8 V at the portal to -12 V at the lower sections of the pocket because the conical structure of the host means that the carboxylates at the rim are further from the C_4 -axis than the four carboxylates in the pendent groups. However, at the very base of the cavity, two factors counter this increase in potential: (1) the bare host structure, i.e., the cone of 12 aromatic rings defining the pocket, has a large dipole (4–

5 D, MMFF) that is colinear with the C_4 -axis and points out of the portal. This is perhaps most evident with the small areas of the weakly negative electrostatic potential (yellow spots in Figure 5) that correspond to H5 atoms of the resorcinol rings; (2) as revealed by electrostatic potential calculations of the hosts themselves,¹⁰⁸ the array of C–H hydrogen-bond donors¹⁰⁹ (H_b in Figure 2) pointing into the lower region of the cavity are relatively electron deficient. Correspondingly, the slight polarization of these C–H bonds contributes to the attenuation of the electrostatic potential in their vicinity (light red areas adjacent to indicated benzal hydrogens).

These electrostatic potential field calculations reveal two important conclusions. First, that the minor difference between hosts **1** and **2**, i.e., the presence of four methyl groups at the rim of the latter, does not significantly change the electrostatic potential within the pocket (Figure 5). These calculations therefore demonstrate that the methyl groups do not directly contribute to the differences in the binding profiles of hosts **1** and **2** (vide infra). Second, the solvation of the pocket and the location of the counter sodium ions of both the host and the guest must play a key role in the ability of **1** and **2** to bind anions. The intrinsic heterogeneity of the field is less unfavorable to anion binding at the base of the pocket and consequently the effects of solvation and counterion must at least uniformly affect the overall field of the host in aqueous solution and potentially modify this intrinsic field in a heterogeneous manner to enhance guest binding at the base of the pocket.

ITC Data for Hosts **1–4.** As Table 1 reveals, even though hosts **1** and **2** only differ in the presence of four methyl groups in the latter, they have quite different anion-binding profiles. Thus, **1** preferentially binds SCN^- , $(CN)_2N^-$, $CNBH_3^-$, and ClO_4^- , whereas **2** preferentially binds PF_6^- , ReO_4^- , TfO^- , and $MeSO_2S^-$. Overall, however, host **2** is the stronger binder. Thus, the range of ΔG° values for **1** is -2.15 to -4.59 kcal mol⁻¹ (av. = -3.22 kcal mol⁻¹); whereas for **2** it is -2.67 to -5.69 kcal mol⁻¹ (av. = -3.82 kcal mol⁻¹). However, the most dramatic differences between the hosts are in the enthalpy and entropy changes associated with anion binding. In all cases, binding to **2** is more exothermic and more entropically penalized, but the extreme case is ReO_4^- . This anion has a preference to bind to **2** of $\Delta\Delta G^\circ = -1.16$ kcal mol⁻¹. However, ITC reveals that when ReO_4^- binds to **2** it releases ~6 kcal mol⁻¹ more heat than when it binds to **1** but suffers from an entropic penalty at room temperature that is more than double that when binding to **1**. It is hard to account for such differences in thermodynamics by invoking host–guest interactions unique to **2** such as Ar–Me…X hydrogen bonds. Similarly, our electrostatic potential calculations do not highlight any significant differences between **1** and **2** that might account for this data.

Table 2 reveals the thermodynamic data for the two cyclodextrins studied. Cyclodextrin **3** is an exceedingly well-studied host capable of binding a wide range of organic guests.¹¹⁰ However, the thermodynamic data for *per*-methylated α -cyclodextrin **4** is far less comprehensive. Where direct comparisons between the two hosts can be made, it is found that **4** binds guests such as benzoic acid or phenol derivatives more strongly, typically 0.5 to 1 kcal mol⁻¹ more strongly.¹¹¹ This has been attributed to the fact that methylation lengthens the cavity and correspondingly makes it less polar; any countering effects of the less preorganized nature of **4** due to the loss of inter-ring hydrogen bonding are not evident.^{112,113}

Table 2 reveals that **4** also binds the studied anions more strongly than host **3**; although the affinities of **3** and **4** sometimes do not differ significantly, in no instance does **3** bind an anionic guest significantly more strongly. Previously, anion association to **3** has been attributed to the hydrogen-bond donor $-\text{OH}$ groups on the rims of the cyclodextrin.^{86,104–107} This may indeed play a role in its binding properties; however, the fact that **4** is devoid of these hydrogen-bond donor groups but binds anions more strongly suggests that other factors are at play. This is underscored by the enthalpy data for **3** and **4**. The hydrogen-bond donor groups of **3** would be expected to significantly contribute to the exothermicity of anion association; however, the reverse is observed here. Removal of the donor groups by methylation leads to stronger binding and an $\sim 60\%$ increase in the exothermicity for binding to **4**.

Of all the anionic guests examined, only four were found to bind to all four hosts **1–4**: CNBH_3^- , ClO_4^- , ReO_4^- , and PF_6^- . The thermodynamics of these processes are compared in Figure 6. Although hosts **1** and **2** mostly bind guests more

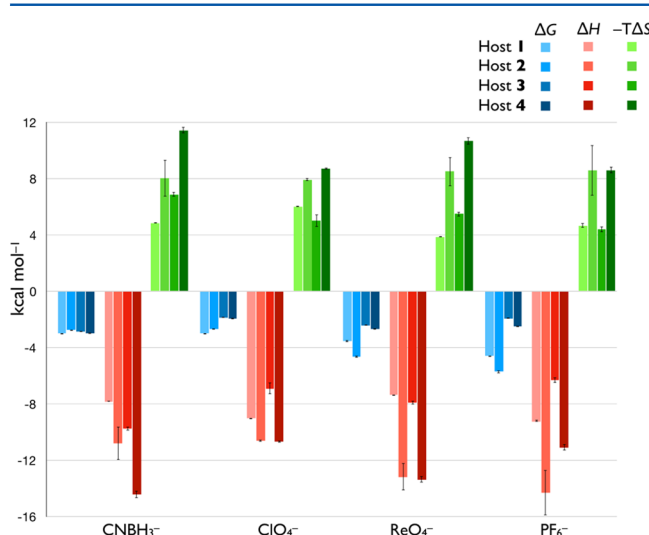


Figure 6. Comparison of the ITC-derived thermodynamic data (ΔG , ΔH , and $-T\Delta S$) of the binding of anion guests CNBH_3^- , ClO_4^- , ReO_4^- , and PF_6^- to hosts **1–4**. The data is arbitrarily organized from weakest to strongest binding guest for host **1**. Error bars are shown (see also Supporting Information).

strongly than **3** and **4**, it is generally host **4** that binds guests with the greatest enthalpy change. Correspondingly, however, binding to host **4** is associated with relatively large entropic penalties. For example, the average entropic penalty associated with binding to hosts **1–4** is, respectively, 4.87, 8.27, 5.45, and 15.34 kcal mol⁻¹.

An inspection of the collated thermodynamic data (Figure 6) reveals puzzles that are hard to explain. Consider for example ReO_4^- versus ClO_4^- . These are similarly sized tetrahedral anions ($V = 59$ and 55 nm^3 respectively), with very different free energies of hydration ($\Delta G_{\text{hyd}} = 80.8$ and $51.1 \text{ kcal mol}^{-1}$ respectively). However, as is revealed in Tables 1 and 2 as well as Figure 6, the free energies of complexation of ReO_4^- to hosts **1–4** are, respectively, -3.51 , -4.67 , -2.41 , and $-2.68 \text{ kcal mol}^{-1}$ (range = $2.26 \text{ kcal mol}^{-1}$). In contrast, more poorly solvated ClO_4^- shows the following affinity to the same hosts: -3.01 , -2.67 , -1.86 , $-1.91 \text{ kcal mol}^{-1}$ (range = $1.16 \text{ kcal mol}^{-1}$). Thus, not only is the more strongly solvated ReO_4^- the better guest for all hosts, but ReO_4^- also shows a greater

sensitivity to its binding environment. This is also evident in the enthalpy and entropy values for binding. For example, for ReO_4^- , the ΔH values associated with binding to hosts **1–4** are -7.39 , -13.19 , -7.90 , and $-13.38 \text{ kcal mol}^{-1}$ (av. = $10.46 \text{ kcal mol}^{-1}$, range = $5.99 \text{ kcal mol}^{-1}$), while for ClO_4^- they are -9.05 , -10.62 , -6.90 , and $-10.69 \text{ kcal mol}^{-1}$ (av. = $9.31 \text{ kcal mol}^{-1}$, range = $3.79 \text{ kcal mol}^{-1}$).

What lies behind these differences? There are two distinct possibilities. Previously, we showed that anion binding to host **1** occurs with only partial desolvation of the anion.⁸¹ Such partial desolvation is a less energy intensive process than the complete removal of the surrounding waters (i.e., $\Delta G^\circ_{\text{hyd}}$), and is analogous to the partial desolvation of anions occurring at the air–water^{30–40} or oil–water interface.^{41–43} The difference with host binding is that complexion of a partially solvated ion must result in some rearrangement of the idealized (partial) solvation shell around the anion to complement the structure of the pocket.¹¹⁴ We suspect that the induced conformation change in the guest ($\text{X}^-(\text{H}_2\text{O})_n$) is different for each host. For example, the difference in binding profile for hosts **1** and **2**, arises in part because the methyl groups of the latter change the nature of the solvation shell of the bound anion. Likewise, the bowl and toroidal shapes of the two classes of hosts must each contribute in their own way to the thermodynamic differences in anion affinities. Unfortunately, this is not currently possible to verify experimentally or computationally; to begin to address this we first have to fully understand the hydration shells of the anions themselves.

In addition it is also likely that the different pockets of hosts **1–4** change the nature of the water bound inside the “free” host.⁹⁵ It is well understood that convex, planar, and concave surfaces are solvated differently⁶⁵ and that each shows its own unique dependency of scale.^{115–120} That this likely has a major impact on the thermodynamics of host–guest complexation can be appreciated if it is recalled that the hydrophobic effect is relative to other solvents, not the gas phase.¹²¹ In other words, as with any solvent, water weakens the intrinsic (gas-phase) interaction between any two surfaces by competing for those surfaces; however, relative to organic solvents, water is not a strong competitor. As a result, binding in water is frequently stronger than comparable systems in nonaqueous media (the hydrophobic effect).

Considering the different possible solvation types of molecular surfaces, it is interesting to consider the possibility of a host templating cavity formation in water. Revised scaled particle theory calculations¹²² as well as an analytical equation of state for cavity formation derived from combined experimental and simulation results,¹²³ reveal that the energy requirement to form a cavity in water equivalent to the volume of host **1** is approximately 25 kcal mol^{-1} . In contrast, the free energy of desolvation of the cavity of **1** has been calculated to be $\sim 5 \text{ kcal mol}^{-1}$.¹²⁴ In other words, a host with a sizable cavity (200 – 300 \AA^3) is at least capable of considerably destabilizing water within its cavity.

The type of behavior exhibited by hosts **1–4**, i.e., that the free energy of guest binding is dominated by enthalpy, has been attributed to this destabilization of solvating waters.^{125–127} This idea behind “high-energy” water, first put forth by Bender,¹²⁸ is that, “water molecules in the cavity cannot form their full complement of hydrogen bonds as a result of steric restrictions”. Thus, when an incoming guest displaces these waters to the bulk they achieve their full complement of hydrogen bonds, with the result that there is a net enthalpy gain

in the system.^{125,127} There is evidently truth in this statement, but the terminology is not ideal. “Energy” means different things to different chemists, and unsurprisingly, there are examples in the literature where “high energy” is used in free energetic and enthalpic terms. Furthermore, since the chemical potentials or partial molar Gibbs free energy of all water molecules in an equilibrated system are necessarily the same, using the term in the context of this standard definition of free energy is misleading. Moreover, “high-energy water” also sidesteps a key issue that the field is not in a position to yet address. How does entropy play into this idea? The binding of water to a restrictive space can greatly reduce its entropy of translation (ΔS_{trans}), but, being unable to form their full complement of hydrogen bonds, such bound waters possess a counteracting increase in their entropy of rotation (ΔS_{rot}). How these different kinds of entropy contribute overall to the free energy of binding is not clear. Relatedly, what if a binding event is entropy driven and dominated? What defines low-entropy water?

Furthermore, describing a binding event as being driven by “high-energy water” sidesteps other factors contributing to guest binding. There is also guest desolvation to consider, and in the context of the work described here, the point that the nature of the guest ($X^-(H_2O)_n$) certainly differs from host to host; bound to a CD, an anionic guest can be solvated by water at both portals, whereas this is not possible when bound to the cavitands. Additionally, there is as yet poorly understood solvation/desolvation relationships based on Gibbs inequalities, e.g., that electrostatic interactions are not expected to contribute to the observed entropy changes of solvation/desolvation (binding) because the large electrostatic solute–solvent and solvent reorganization entropies are canceling.^{129,130}

These problems can be largely avoided (at least until we have a better understanding) if a thermodynamic definition of pocket solvation is avoided. Thus, an alternative perspective is to view the solvation of nonpolar concavity in terms of drying transitions or dewetting. As a function of time, the solvation of a concavity fluctuates between a maximum and minimum (and other intermediate solvation states), and it is the probability of the cavity being in a certain solvation state that readily defines these systems. Drying transitions have been repeatedly observed in silico: in the study of water between hydrophobic plates as well as in carbon nanotubes and protein cavities.^{117,118,131,132} However, there is only a small amount^{120,133} of (indirect) empirical evidence of their existence. Nevertheless, the general concept is intriguing from a supramolecular perspective. To paraphrase Cram, the structure of host such as **1** prepays the free energy costs to promote formation of a cavity within water; in essence, hosts may function as an antitemplate to promote the formation of nothingness in what is an exceedingly small solvent capable of solvating the tightest of surfaces.

CONCLUSIONS

NMR spectroscopy and ITC studies have confirmed that polarizable anions have a general affinity for nonpolar concavities. For the two classes of host examined, affinity follows the Hofmeister series, with the more enveloping hosts **1** and **2** possessing the less polar pockets and demonstrating stronger associations. This is despite the fact that the cavitand hosts possess intrinsic negative electrostatic fields that would be expected to repel anions. The fact that these hosts do bind

anions, and the observation that the four hosts each possess specific anion affinities that cannot be readily explained by their structures, point to the importance of counter cations and the solvation of the “empty” pockets, the free guests, and the host–guest complexes. Thus, future progress in understanding the Hofmeister effect must therefore include appreciating the relationship between concavity shape and size and drying transitions as well as building a detailed picture of the solvation differences of the free and bound anionic guests.

EXPERIMENTAL SECTION

Full experimental details can be found in the [Supporting Information](#). All salts (purity $\geq 99\%$) and host **3** (α -cyclodextrin) were purchased from Aldrich Chemical Co. or Acros Organics and were used without further purification. Hosts **1**,⁸¹ **2**,^{83,84} and **4**⁸⁵ were synthesized as previously reported. All ^1H NMR spectra were recorded on a Bruker 500 MHz spectrometer, regulated at 298 K. Spectral processing was carried out using Mnova software (Mestrelab Research S.L.). All titrations utilized D_2O (Cambridge Isotopes, 99.9%+), with solutions freshly prepared on the day of each titration. Isothermal Titration Calorimetric (ITC) experiments of hosts **2**–**4** with the selected salts were performed at 298 K using a VP-ITC MicroCalorimeter from Microcal, U.S.A.

ASSOCIATED CONTENT

Supporting Information

The Supporting Information is available free of charge on the [ACS Publications website](#) at DOI: [10.1021/acs.jpcb.7b12259](https://doi.org/10.1021/acs.jpcb.7b12259).

Experimental procedures; summary of thermodynamic data; NMR and ITC data; and electrostatic potential calculations ([PDF](#))

AUTHOR INFORMATION

Corresponding Author

*E-mail: bgibb@tulane.edu; Phone: (504) 862-8136

ORCID

Henry S Ashbaugh: [0000-0001-9869-1900](https://orcid.org/0000-0001-9869-1900)

Bruce C. Gibb: [0000-0002-4478-4084](https://orcid.org/0000-0002-4478-4084)

Author Contributions

[§]M.R.S. and W.Y. contributed equally to this paper.

Notes

The authors declare no competing financial interest.

ACKNOWLEDGMENTS

The authors gratefully acknowledge the support of the National Institutes of Health (GM 098141) for funding this study.

REFERENCES

- (1) Hofmeister, F. Zur Lehre Von Der Wirkung Der Salze. *Naunyn-Schmiedeberg's Arch. Pharmacol.* **1888**, *24*, 247–260.
- (2) Hofmeister, F. Zur Lehre Von Der Wirkung Der Salze. *Naunyn-Schmiedeberg's Arch. Pharmacol.* **1888**, *25*, 1–30.
- (3) Kunz, W.; Henle, J.; Ninham, B. W. Zur Lehre Von Der Wirkung Der Salze” (About the Science of the Effect of Salts): Franz Hofmeister’s Historical Papers. *Curr. Opin. Colloid Interface Sci.* **2004**, *9* (1–2), 19–37.
- (4) Gilliland, G. L.; Tung, M.; Ladner, J. The Biological Macromolecule Crystallization Database and Nasa Protein Crystal Growth Archive. *J. Res. Natl. Inst. Stand. Technol.* **1996**, *101*, 309.
- (5) von Hippel, P.; Wong, K.-Y. On the Conformational Stability of Globular Proteins. The Effects of Various Electrolytes and Non-

- electrolytes on the Thermal Ribonuclease Transition. *J. Bio. Chem.* **1965**, *240*, 3909–3923.
- (6) Collins, K. D.; Washabaugh, M. W. The Hofmeister Effect and the Behavior of Water at Interfaces. *Q. Rev. Biophys.* **1985**, *18*, 323–422.
- (7) Gurney, R. W. *Ionic Processes in Solution*; McGraw-Hill: New York, 1953.
- (8) Fajans, K.; Johnson, O. Apparent Volumes of Individual Ions in Aqueous Solution. *J. Am. Chem. Soc.* **1942**, *64*, 668–698.
- (9) Gibson, R. E. The Influence of Concentration on the Compressions of Aqueous Solutions of Certain Sulfates and a Note on the Representation of the Compressions of Aqueous Solutions as a Function of Pressure. *J. Am. Chem. Soc.* **1934**, *56*, 4–14.
- (10) Jenkins, H. D. B.; Marcus, Y. Viscosity B-Coefficients of Ions in Solution. *Chem. Rev.* **1995**, *95*, 2695–2724.
- (11) Jones, G.; Dole, M. The Viscosity of Aqueous Solutions of Strong Electrolytes with Special Reference to Barium Chloride. *J. Am. Chem. Soc.* **1929**, *51*, 2950–2964.
- (12) Cox, W. M.; Wolfenden, J. H. The Viscosity of Strong Electrolytes Measured by a Differential Method. *Proc. R. Soc. London, Ser. A* **1934**, *145* (855), 475–488.
- (13) Bello, J.; Bello, H. R. Interactions of Model Peptides with Water and Lithium Bromide. *Nature* **1961**, *190*, 440–441.
- (14) Long, F. A.; McDevit, W. F. Activity Coefficients of Non-Electrolyte Solutes in Aqueous Salt Solutions. *Chem. Rev.* **1952**, *51*, 119–169.
- (15) Kebarle, P.; Arshadi, M.; Scarborough, J. Comparison of Individual Hydration Energies for Positive and Negative Ions on the Basis of Gas-Phase Hydration Experiments. *J. Chem. Phys.* **1969**, *50* (2), 1049.
- (16) Onsager, L.; Samaras, N. N. T. The Surface Tension of Debye-Hückel Electrolytes. *J. Chem. Phys.* **1934**, *2* (8), 528.
- (17) Jones, G.; Ray, W. A. The Surface Tension of Solutions of Electrolytes as a Function of the Concentration. I. A Differential Method for Measuring Relative Surface Tension. *J. Am. Chem. Soc.* **1937**, *59*, 187–198.
- (18) Jarvis, N. L.; Scheiman, M. A. Surface Potentials of Aqueous Electrolyte Solutions. *J. Phys. Chem.* **1968**, *72*, 74–78.
- (19) von Hippel, P.; Petricolas, V.; Schack, L.; Karlson, L. Model Studies on the Effects of Neutral Salts on the Conformational Stability of Biological Macromolecules. I. Ion Binding to Polyacrylamide and Polystyrene Columns. *Biochemistry* **1973**, *12*, 1256–1264.
- (20) Jungwirth, P.; Cremer, P. S. Beyond Hofmeister. *Nat. Chem.* **2014**, *6* (4), 261–3.
- (21) Tielrooij, K. J.; Garcia-Araez, N.; Bonn, M.; Bakker, H. J. Cooperativity in Ion Hydration. *Science* **2010**, *328*, 1006–1009.
- (22) Omata, A. W.; Kropman, M. F.; Woutersen, S.; Bakker, H. J. Negligible Effect of Ions on the Hydrogen-Bond Structure in Liquid Water. *Science* **2003**, *301*, 347–349.
- (23) van der Post, S. T.; Scheidelaar, S.; Bakker, H. J. Water Dynamics in Aqueous Solutions of Tetra-N-Alkylammonium Salts: Hydrophobic and Coulomb Interactions Disentangled. *J. Phys. Chem. B* **2013**, *117* (48), 15101–10.
- (24) Moilanen, D. E.; Wong, D.; Rosenfeld, D. E.; Fenn, E. E.; Fayer, M. D. Ion-Water Hydrogen-Bond Switching Observed with 2d Ir Vibrational Echo Chemical Exchange Spectroscopy. *Proc. Natl. Acad. Sci. U. S. A.* **2009**, *106* (2), 375–380.
- (25) Turton, D. A.; Hunger, J.; Hefta, G.; Buchner, R.; Wynne, K. Glasslike Behavior in Aqueous Electrolyte Solutions. *J. Chem. Phys.* **2008**, *128* (16), 161102.
- (26) Wachter, W.; Kunz, W.; Buchner, R.; Hefta, G. Is There an Anionic Hofmeister Effect on Water Dynamics? Dielectric Spectroscopy of Aqueous Solutions of NaBr, NaI, NaNO₃, NaClO₄, and NaSCN. *J. Phys. Chem. A* **2005**, *109*, 8675–8683.
- (27) Smith, J. D.; Saykally, R. J.; Geissler, P. L. The Effects of Dissolved Halide Anions on Hydrogen Bonding in Liquid Water. *J. Am. Chem. Soc.* **2007**, *129*, 13847–13856.
- (28) Perera, P.; Wyche, M.; Loethen, Y.; Ben-Amotz, D. Solute-Induced Perturbations of Solvent-Shell Molecules Observed Using Multivariate Raman Curve Resolution. *J. Am. Chem. Soc.* **2008**, *130* (14), 4576–4577.
- (29) Funkner, S.; Niehues, G.; Schmidt, D. A.; Heyden, M.; Schwaab, G.; Callahan, K. M.; Tobias, D. J.; Havenith, M. Watching the Low-Frequency Motions in Aqueous Salt Solutions: The Terahertz Vibrational Signatures of Hydrated Ions. *J. Am. Chem. Soc.* **2012**, *134* (2), 1030–5.
- (30) Petersen, P. B.; Saykally, R. J. On the Nature of Ions at the Liquid Water Surface. *Annu. Rev. Phys. Chem.* **2006**, *57*, 333–64.
- (31) Verreault, D.; Allen, H. C. Bridging the Gap between Microscopic and Macroscopic Views of Air/Aqueous Salt Interfaces. *Chem. Phys. Lett.* **2013**, *586*, 1–9.
- (32) Petersen, P. B.; Saykally, R. J. Adsorption of Ions to the Surface of Dilute Electrolyte Solutions: The Jones-Ray Effect Revisited. *J. Am. Chem. Soc.* **2005**, *127*, 15446–15452.
- (33) Petersen, P. B.; Johnson, J. C.; Knutsen, K. P.; Saykally, R. J. Direct Experimental Validation of the Jones-Ray Effect. *Chem. Phys. Lett.* **2004**, *397* (1–3), 46–50.
- (34) Petersen, P. B.; Saykally, R. J. Confirmation of Enhanced Anion Concentration at the Liquid Water Surface. *Chem. Phys. Lett.* **2004**, *397* (1–3), 51–55.
- (35) Liu, D. R.; Ma, G.; Levering, L. M.; Allen, H. C. Vibrational Spectroscopy of Aqueous Sodium Halide Solutions and Air-Liquid Interfaces: Observation of Increased Interfacial Depth. *J. Phys. Chem. B* **2004**, *108*, 2252–2260.
- (36) Raymond, E. A.; Richmond, G. L. Probing the Molecular Structure and Bonding of the Surface of Aqueous Salt Solutions. *J. Phys. Chem. B* **2004**, *108*, 5051–5059.
- (37) Pegram, L. M.; Record, M. T. J. Hofmeister Salt Effects on Surface Tension Arise from Partitioning of Anions and Cations between Bulk Water and the Air-Water Interface. *J. Phys. Chem. B* **2007**, *111*, 5411–5417.
- (38) Petersen, P. B.; Saykally, R. J.; Mucha, M.; Jungwirth, P. Enhanced Concentration of Polarizable Anions at the Liquid Water Surface: SHG Spectroscopy and MD Simulations of Sodium Thiocyanide. *J. Phys. Chem. B* **2005**, *109*, 10915–10921.
- (39) Jungwirth, P.; Tobias, J. W. Specific Ion Effects at the Air/Water Interface. *Chem. Rev.* **2006**, *106*, 1259–1281.
- (40) Jungwirth, P.; Tobias, D. J. Ions at the Air/Water Interface. *J. Phys. Chem. B* **2002**, *106*, 6361–6373.
- (41) Luo, G.; Malkova, S.; Yoon, J.; Schultz, D. G.; Lin, B.; Meron, M.; Benjamin, I.; Vanysek, P.; Schlossman, M. L. Ion Distributions near a Liquid-Liquid Interface. *Science* **2006**, *311* (5758), 216–218.
- (42) Vazdar, M.; Pluharova, E.; Mason, P. E.; Vacha, R.; Jungwirth, P. Ions at Hydrophobic Aqueous Interfaces: Molecular Dynamics with Effective Polarization. *J. Phys. Chem. Lett.* **2012**, *3* (15), 2087–2091.
- (43) Scheu, R.; Chen, Y.; Subinya, M.; Roke, S. Stern Layer Formation Induced by Hydrophobic Interactions: A Molecular Level Study. *J. Am. Chem. Soc.* **2013**, *135* (51), 19330–19335.
- (44) Okur, H. I.; Hladíková, J.; Rembert, K. B.; Cho, Y.; Heyda, J.; Dzubiella, J.; Cremer, P. S.; Jungwirth, P. Beyond the Hofmeister Series: Ion-Specific Effects on Proteins and Their Biological Functions. *J. Phys. Chem. B* **2017**, *121* (9), 1997–2014.
- (45) Zhang, Y. J.; Cremer, P. S. Chemistry of Hofmeister Anions and Osmolytes. *Annu. Rev. Phys. Chem.* **2010**, *61*, 63–83.
- (46) Zhang, Y.; Furyk, S.; Bergbreiter, D. E.; Cremer, P. S. Specific Ion Effects on the Water Solubility of Macromolecules: PNIPAM and the Hofmeister Series. *J. Am. Chem. Soc.* **2005**, *127*, 14505–14510.
- (47) Zhang, Y.; Cremer, P. S. Interactions between Macromolecules and Ions: The Hofmeister Series. *Curr. Opin. Chem. Biol.* **2006**, *10*, 658–663.
- (48) Rembert, K. B.; Paterova, J.; Heyda, J.; Hilty, C.; Jungwirth, P.; Cremer, P. S. Molecular Mechanisms of Ion-Specific Effects on Proteins. *J. Am. Chem. Soc.* **2012**, *134* (24), 10039–46.
- (49) Paterová, J.; Rembert, K. B.; Heyda, J.; Kurra, Y.; Okur, H. I.; Liu, W. R.; Hilty, C.; Cremer, P. S.; Jungwirth, P. Reversal of the Hofmeister Series: Specific Ion Effects on Peptides. *J. Phys. Chem. B* **2013**, *117* (27), 8150–8.

- (50) Pegram, L. M.; Record, M. T. J. Quantifying Accumulation or Exclusion of H^+ , HO^- , and Hofmeister Salt Ions near Interfaces. *Chem. Phys. Lett.* **2008**, *467*, 1–8.
- (51) Xie, W. J.; Gao, Y. Q. A Simple Theory for the Hofmeister Series. *J. Phys. Chem. Lett.* **2013**, *4*, 4247–4252.
- (52) Gao, Y. Q. Simple Theory for Salt Effects on the Solubility of Amide. *J. Phys. Chem. B* **2012**, *116*, 9934–9943.
- (53) Jungwirth, P.; Winter, B. Ions at Aqueous Interfaces: From Water Surface to Hydrated Proteins. *Annu. Rev. Phys. Chem.* **2008**, *59*, 343–66.
- (54) Zangi, R.; Hagen, M.; Berne, B. J. Effect of Ions on the Hydrophobic Interaction between Two Plates. *J. Am. Chem. Soc.* **2007**, *129*, 4678–4686.
- (55) van der Vegt, N. F.; Haldrup, K.; Roke, S.; Zheng, J.; Lund, M.; Bakker, H. J. Water-Mediated Ion Pairing: Occurrence and Relevance. *Chem. Rev.* **2016**, *116* (13), 7626–41.
- (56) Jungwirth, P. Ion Pairing: From Water Clusters to the Aqueous Bulk. *J. Phys. Chem. B* **2014**, *118*, 10333.
- (57) Minofar, B.; Vacha, R.; Wahab, A.; Mahiuddin, S.; Kunz, W.; Jungwirth, P. Propensity for the Air/Water Interface and Ion Pairing in Magnesium Acetate Vs Magnesium Nitrate Solutions: Molecular Dynamics Simulations and Surface Tension Measurements. *J. Phys. Chem. B* **2006**, *110* (32), 15939–44.
- (58) Marcus, Y.; Hefter, G. Ion Pairing. *Chem. Rev.* **2006**, *106* (11), 4585–621.
- (59) Kebarle, P. Ion Thermochemistry and Solvation from Gas Phase Ion Equilibria. *Annu. Rev. Phys. Chem.* **1977**, *28*, 445–476.
- (60) Marcus, Y. Effect of Ions on the Structure of Water: Structure Making and Breaking. *Chem. Rev.* **2009**, *109* (3), 1346–70.
- (61) Dalleska, N. F.; Honma, K.; Sunderlin, L. S.; Armentrout, P. B. Solvation of Transition Metal Ions by Water. Sequential Binding Energies of $\text{M}^+(\text{H}_2\text{O})_x$ ($X = 1\text{--}4$) for $\text{M} = \text{Ti}$ to Cu Determined by Collision-Induced Dissociation. *J. Am. Chem. Soc.* **1994**, *116*, 3519–3528.
- (62) Robertson, W. H.; Johnson, M. A. Molecular Aspects of Halide Ion Hydration: The Cluster Approach. *Annu. Rev. Phys. Chem.* **2003**, *54*, 173–213.
- (63) O'Brien, J. T.; Prell, J. S.; Bush, M. F.; Williams, E. R. Sulfate Ion Patterns Water at Long Distance. *J. Am. Chem. Soc.* **2010**, *132* (24), 8248–8249.
- (64) Garand, E.; Wende, T.; Goebbert, D. J.; Bergmann, R.; Meijer, G.; Neumark, D. M.; Asmis, K. R. Infrared Spectroscopy of Hydrated Bicarbonate Anion Clusters: $\text{HCO}_3^-(\text{H}_2\text{O})_{1\text{--}10}$. *J. Am. Chem. Soc.* **2010**, *132* (2), 849–56.
- (65) Hillyer, M. B.; Gibb, B. C. Molecular Shape and the Hydrophobic Effect. *Annu. Rev. Phys. Chem.* **2016**, *67*, 307–29.
- (66) McDermott, M. L.; Vanselous, H.; Corcelli, S. A.; Petersen, P. B. Dna's Chiral Spine of Hydration. *ACS Cent. Sci.* **2017**, *3* (7), 708–714.
- (67) Heyda, J.; Hrobarik, T.; Jungwirth, P. Ion-Specific Interactions between Halides and Basic Amino Acids in Water. *J. Phys. Chem. A* **2009**, *113* (10), 1969–75.
- (68) Watson, J. D.; Milner-White, E. J. A Novel Main-Chain Anion-Binding Site in Proteins: The Nest. A Particular Combination of F, C Values in Successive Residues Gives Rise to Anion-Binding Sites That Occur Commonly and Are Found Often at Functionally Important Regions. *J. Mol. Biol.* **2002**, *315*, 171–182.
- (69) Denessiouk, K. A.; Johnson, M. S.; Denesyuk, A. I. Novel C^aNN Structural Motif for Protein Recognition of Phosphate Ions. *J. Mol. Biol.* **2005**, *345* (3), 611–29.
- (70) Crevenna, A. H.; Naredi-Rainer, N.; Lamb, D. C.; Wedlich-Soldner, R.; Dzubiella, J. Effects of Hofmeister Ions on the Alpha-Helical Structure of Proteins. *Biophys. J.* **2012**, *102* (4), 907–15.
- (71) Flores, S. C.; Kherb, J.; Cremer, P. S. Direct and Reverse Hofmeister Effects on Interfacial Water Structure. *J. Phys. Chem. C* **2012**, *116* (27), 14408–14413.
- (72) Dzubiella, J. Salt-Specific Stability of Short and Charged Alanine-Based α -Helices. *J. Phys. Chem. B* **2009**, *113* (52), 16689–16694.
- (73) Dzubiella, J. Salt-Specific Stability and Denaturation of a Short Salt-Bridge-Forming Alpha-Helix. *J. Am. Chem. Soc.* **2008**, *130* (42), 14000–7.
- (74) Harries, D.; Rau, D. C.; Parsegian, V. A. Solutes Probe Hydration in Specific Association of Cyclodextrin and Adamantane. *J. Am. Chem. Soc.* **2005**, *127*, 2184–2190.
- (75) Pegram, L. M.; Wendorff, T.; Erdmann, R.; Shkel, I.; Bellissimo, D.; Felitsky, D. J.; Record, M. T. J. Why Hofmeister Effects of Many Salts Favor Protein Folding but Not DNA Helix Formation. *Proc. Natl. Acad. Sci. U. S. A.* **2010**, *107*, 7716–7721.
- (76) Pegram, L. M.; Record, M. T. J. Thermodynamic Origin of Hofmeister Ion Effects. *J. Phys. Chem. B* **2008**, *112*, 9428–9436.
- (77) Fox, J. M.; Kang, K.; Sherman, W.; Heroux, A.; Sastry, G. M.; Baghbanzadeh, M.; Lockett, M. R.; Whitesides, G. M. Interactions between Hofmeister Anions and the Binding Pocket of a Protein. *J. Am. Chem. Soc.* **2015**, *137* (11), 3859–66.
- (78) Rother, K.; Preissner, R.; Goede, A.; Frömmel, C. Inhomogeneous Molecular Density: Reference Packing Densities and Distribution of Cavities within Proteins. *Bioinformatics* **2003**, *19* (16), 2112–2121.
- (79) Gibb, C. L. D.; Gibb, B. C. Anion Binding to Hydrophobic Concavity Is Central to the Salting-in Effects of Hofmeister Chaotropes. *J. Am. Chem. Soc.* **2011**, *133* (19), 7344–7347.
- (80) Gibb, C. L.; Oertling, E. E.; Velaga, S.; Gibb, B. C. Thermodynamic Profiles of Salt Effects on a Host-Guest System: New Insight into the Hofmeister Effect. *J. Phys. Chem. B* **2015**, *119* (17), 5624–38.
- (81) Sokkalingam, P.; Shraberger, J.; Rick, S. W.; Gibb, B. C. Binding Hydrated Anions with Hydrophobic Pockets. *J. Am. Chem. Soc.* **2016**, *138* (1), 48–51.
- (82) Carnegie, R.; Gibb, C. L. D.; Gibb, B. C. Anion Complexation and the Hofmeister Effect. *Angew. Chem., Int. Ed.* **2014**, *53* (43), 11498–11500.
- (83) Gan, H.; Benjamin, C. J.; Gibb, B. C. Nonmonotonic Assembly of a Deep-Cavity Cavitand. *J. Am. Chem. Soc.* **2011**, *133*, 4770–4773.
- (84) Gan, H.; Gibb, B. C. Guest-Mediated Switching of the Assembly State of a Water-Soluble Deep-Cavity Cavitand. *Chem. Commun.* **2013**, *49*, 1395–1397.
- (85) Szejtli, J.; Liptak, A.; Jodal, I.; Fugedi, P.; Nanasi, P.; Neszmelyi, A. Synthesis and Carbon-13 Nmr Spectroscopy of Methylated β -Cyclodextrins. *Starch - Stärke* **1980**, *32* (5), 165–169.
- (86) Matsui, Y.; Ono, M.; Tokunaga, S. NMR Spectroscopy of Cyclodextrin-Inorganic Anion Systems. *Bull. Chem. Soc. Jpn.* **1997**, *70* (3), 535–541.
- (87) Turnbull, W. B.; Daranas, A. H. On the Value of c: Can Low Affinity Systems be studied by Isothermal Titration Calorimetry? *J. Am. Chem. Soc.* **2003**, *125*, 14859–14866.
- (88) Tellinghuisen, J. Isothermal Titration Calorimetry at Very Low c Anal. *Anal. Biochem.* **2008**, *373*, 395–397.
- (89) Jakalian, A.; Bush, B. L.; Jack, D. B.; Bayly, C. I. Fast, Efficient Generation of High-Quality Atomic Charges. AM1-BCC Model: I. Method. *J. Comput. Chem.* **2000**, *21* (2), 132–146.
- (90) Wanjari, P. P.; Gibb, B. C.; Ashbaugh, H. S. Simulation Optimization of Spherical Non-Polar Guest Recognition by Deep-Cavity Cavitands. *J. Chem. Phys.* **2013**, *139* (23), 234502.
- (91) Sullivan, M. R.; Sokkalingam, P.; Nguyen, T.; Donahue, J. P.; Gibb, B. C. Binding of Carboxylate and Trimethylammonium Salts to Octa-Acid and Temoa Deep-Cavity Cavitands. *J. Comput.-Aided Mol. Des.* **2017**, *31* (1), 21–28.
- (92) Steiner, T.; Saenger, W. Crystal Structure of Anhydrous Hexakis-(2,3,6-Tri-O-Methyl)-Cyclomaltohexaose (Permethyl- α -Cyclodextrin) Grown from Hot Water and from Cold NaCl Solutions. *Carbohydr. Res.* **1996**, *282*, 53–63.
- (93) Sun, H.; Gibb, C. L. D.; Gibb, B. C. Calorimetric Analysis of the 1:1 Complexes Formed between a Water-Soluble Deep-Cavity Cavitand, and Cyclic and Acyclic Carboxylic Acids. *Supramol. Chem.* **2008**, *20* (1-2), 141–147.

- (94) Gibb, C. L. D.; Gibb, B. C. Binding of Cyclic Carboxylates to Octa-Acid Deep-Cavity Cavitand. *J. Comput.-Aided Mol. Des.* **2014**, *28* (4), 319–25.
- (95) Ewell, J.; Gibb, B. C.; Rick, S. W. Water inside a Hydrophobic Cavitand Molecule. *J. Phys. Chem. B* **2008**, *112*, 10272–10279.
- (96) Jana, M.; Bandyopadhyay, S. Hydration Properties of α , β -, and γ -Cyclodextrins from Molecular Dynamics Simulations. *J. Phys. Chem. B* **2011**, *115* (19), 6347–6357.
- (97) Wagner, B. D.; MacDonald, P. J. The Fluorescence Enhancement of 1-Anilinonaphthalene-8-Sulfonate (Ans) by Modified β -Cyclodextrins. *J. Photochem. Photobiol., A* **1998**, *114*, 151–157.
- (98) Pereira-Vilar, A.; Martin-Pastor, M.; Pescego, M.; Garcia-Rio, L. Supramolecular Recognition Induces Nonsynchronous Change of Dye Fluorescence Properties. *J. Org. Chem.* **2016**, *81* (15), 6587–95.
- (99) Dsouza, R. N.; Pischel, U.; Nau, W. M. Fluorescent Dyes and Their Supramolecular Host/Guest Complexes with Macrocycles in Aqueous Solution. *Chem. Rev.* **2011**, *111* (12), 7941–80.
- (100) Jordan, J. H.; Gibb, B. C. Molecular Containers Assembled through the Hydrophobic Effect. *Chem. Soc. Rev.* **2015**, *44* (2), 547–85.
- (101) Assaf, K. I.; Ural, M. S.; Pan, F.; Georgiev, T.; Simova, S.; Rissanen, K.; Gabel, D.; Nau, W. M. Water Structure Recovery in Chaotropic Anion Recognition: High-Affinity Binding of Dodecaborate Clusters to γ -Cyclodextrin. *Angew. Chem., Int. Ed.* **2015**, *54* (23), 6852–6.
- (102) Thoma, J. A.; French, D. Studies on the Schardinger Dextrans. X. The Interaction of Cyclohexaamyllose, Iodine and Iodide. Part I. Spectrophotometric Studies. *J. Am. Chem. Soc.* **1958**, *80*, 6142–6146.
- (103) French, D. The Schardinger Dextrans. *Advances in Carbohydrate Chemistry* **1957**, *12*, 189–260.
- (104) Wojcik, J. F.; Rohrbach, R. P. Small Anion Binding to Cycloamylose. Equilibrium Constants. *J. Phys. Chem.* **1975**, *79*, 2251–2253.
- (105) Gelb, R. I.; Schwartz, L. M.; Radeos, M.; Laufer, D. A. Cycloamylose Complexation of Inorganic Anions. *J. Phys. Chem.* **1983**, *87*, 3349–3354.
- (106) Taraszewska, J.; Wójcik, J. Complexation of Inorganic Anions by β -Cyclodextrin Studied by Polarography And ^1H NMR. *Supramol. Chem.* **1993**, *2* (4), 337–343.
- (107) Godínez, L. A.; Schulze-fiehn, B. G.; Patel, S.; Criss, C. M.; Evanseck, J. D.; Kaifer, A. E. Observation and Interpretation of Anomalous Inorganic Anion Binding with A- and B-Cyclodextrins in Aqueous Media. *Supramol. Chem.* **1996**, *8* (1), 17–22.
- (108) Laughrey, Z. R.; Upton, T. G.; Gibb, B. C. A Deuterated Deep-Cavity Cavitand Confirms the Importance of C-H \cdots X-R Hydrogen Bonds in Guest Binding. *Chem. Commun.* **2006**, *9*, 970–972.
- (109) Gibb, C. L. D.; Stevens, E. D.; Gibb, B. C. C-H \cdots X-R Hydrogen Bonds Drive the Complexation Properties of a Nano-Scale Molecular Basket. *J. Am. Chem. Soc.* **2001**, *123*, 5849–5850.
- (110) Crini, G. Review: A History of Cyclodextrins. *Chem. Rev.* **2014**, *114* (21), 10940–75.
- (111) Rekharsky, M. V.; Inoue, Y. Complexation Thermodynamics of Cyclodextrins. *Chem. Rev.* **1998**, *98*, 1875–1917.
- (112) Harata, K.; Uekama, K.; Otagiri, M.; Hirayama, F. Conformation of Permethylated Cyclodextrins and the Host-Guest Geometry of Their Inclusion Complexes. *J. Inclusion Phenom.* **1984**, *1* (3), 279–93.
- (113) Kano, K.; Ishimura, T.; Negi, S. Mechanism for Binding to the Flexible Cavity of Permethylated A-Cyclodextrin. *J. Inclusion Phenom. Mol. Recognit. Chem.* **1995**, *22* (4), 285–98.
- (114) Marcus, Y. *Ion Properties*, 1st ed.; Marcel Dekker: New York, 1997.
- (115) Rasaiah, J. C.; Garde, S.; Hummer, G. Water in Nonpolar Confinement: From Nanotubes to Proteins and Beyond. *Annu. Rev. Phys. Chem.* **2008**, *59*, 713–40.
- (116) Patel, A. J.; Varilly, P.; Chandler, D.; Garde, S. Quantifying Density Fluctuations in Volumes of All Shapes and Sizes Using Indirect Umbrella Sampling. *J. Stat. Phys.* **2011**, *145* (2), 265–275.
- (117) Berne, B. J.; Weeks, J. D.; Zhou, R. Dewetting and Hydrophobic Interaction in Physical and Biological Systems. *Annu. Rev. Phys. Chem.* **2009**, *60*, 85–103.
- (118) Young, T.; Hua, L.; Huang, X.; Abel, R.; Friesner, R.; Berne, B. J. Dewetting Transitions in Protein Cavities. *Proteins: Struct., Funct., Genet.* **2010**, *78* (8), 1856–1869.
- (119) Wang, L.; Berne, B. J.; Friesner, R. A. Ligand Binding to Protein-Binding Pockets with Wet and Dry Regions. *Proc. Natl. Acad. Sci. U. S. A.* **2011**, *108* (4), 1326–30.
- (120) Yin, H.; Hummer, G.; Rasaiah, J. C. Metastable Water Clusters in the Nonpolar Cavities of the Thermostable Protein Tetrabrachion. *J. Am. Chem. Soc.* **2007**, *129* (23), 7369–7377.
- (121) Ben-Amotz, D. Water-Mediated Hydrophobic Interactions. *Annu. Rev. Phys. Chem.* **2016**, *67*, 617–38.
- (122) Ashbaugh, H.; Pratt, L. Colloquium: Scaled Particle Theory and the Length Scales of Hydrophobicity. *Rev. Mod. Phys.* **2006**, *78* (1), 159–178.
- (123) Ben-Amotz, D. Global Thermodynamics of Hydrophobic Cavitation, Dewetting, and Hydration. *J. Chem. Phys.* **2005**, *123* (18), 184504.
- (124) Olano, L. R.; Rick, S. W. Hydration Free Energies and Entropies for Water in Protein Interiors. *J. Am. Chem. Soc.* **2004**, *126* (25), 7991–8000.
- (125) Biedermann, F.; Nau, W. M.; Schneider, H. J. The Hydrophobic Effect Revisited—Studies with Supramolecular Complexes Imply High-Energy Water as a Noncovalent Driving Force. *Angew. Chem., Int. Ed.* **2014**, *53* (42), 11158–71.
- (126) Biedermann, F.; Vendruscolo, M.; Scherman, O. A.; De Simone, A.; Nau, W. M. Cucurbit[8]Uril and Blue-Box: High-Energy Water Release Overwhelms Electrostatic Interactions. *J. Am. Chem. Soc.* **2013**, *135* (39), 14879–88.
- (127) Biedermann, F.; Uzunova, V. D.; Scherman, O. A.; Nau, W. M.; De Simone, A. Release of High-Energy Water as an Essential Driving Force for the High-Affinity Binding of Cucurbit[n]urils. *J. Am. Chem. Soc.* **2012**, *134* (37), 15318–23.
- (128) VanEtten, R. L.; Sebastian, J. F.; Clowes, G. A.; Bender, M. L. Acceleration of Phenyl Ester Cleavage by Cycloamyloses. A Model for Enzymatic Specificity. *J. Am. Chem. Soc.* **1967**, *89*, 3242.
- (129) Ben-Amotz, D.; Underwood, R. Unraveling Water's Entropic Mysteries: A Unified View of Nonpolar, Polar, and Ionic Hydration. *Acc. Chem. Res.* **2008**, *41* (8), 957–67.
- (130) Ben-Naim, A. *Solvation Thermodynamics*; Springer, 1987.
- (131) Jamadagni, S. N.; Godawat, R.; Garde, S. Hydrophobicity of Proteins and Interfaces: Insights from Density Fluctuations. *Annu. Rev. Chem. Biomol. Eng.* **2011**, *2*, 147–71.
- (132) Patel, A. J.; Varilly, P.; Jamadagni, S. N.; Hagan, M. F.; Chandler, D.; Garde, S. Sitting at the Edge: How Biomolecules Use Hydrophobicity to Tune Their Interactions and Function. *J. Phys. Chem. B* **2012**, *116* (8), 2498–503.
- (133) Qvist, J.; Davidovic, M.; Hamelberg, D.; Halle, B. A Dry Ligand-Binding Cavity in a Solvated Protein. *Proc. Natl. Acad. Sci. U. S. A.* **2008**, *105* (17), 6296–6301.